

## Sub-picosecond dynamics in liquid Si

This article has been downloaded from IOPscience. Please scroll down to see the full text article.

2003 J. Phys.: Condens. Matter 15 L623

(<http://iopscience.iop.org/0953-8984/15/40/L03>)

View [the table of contents for this issue](#), or go to the [journal homepage](#) for more

Download details:

IP Address: 171.66.16.125

The article was downloaded on 19/05/2010 at 15:16

Please note that [terms and conditions apply](#).

## LETTER TO THE EDITOR

**Sub-picosecond dynamics in liquid Si**

**S Hosokawa<sup>1,4</sup>, W-C Pilgrim<sup>1</sup>, Y Kawakita<sup>2</sup>, K Ohshima<sup>2</sup>,  
S Takeda<sup>2</sup>, D Ishikawa<sup>3,5</sup>, S Tsutsui<sup>3</sup>, Y Tanaka<sup>3</sup> and  
A Q R Baron<sup>3</sup>**

<sup>1</sup> Institut für Physikalische-, Kern-, und Makromolekulare Chemie, Philipps Universität Marburg, D-35032 Marburg, Germany

<sup>2</sup> Department of Physics, Faculty of Sciences, Kyushu University, Fukuoka 810-8560, Japan

<sup>3</sup> Spring-8, Hyogo 679-5198, Japan

E-mail: hosokawa@mail.uni-marburg.de

Received 18 June 2003, in final form 28 August 2003

Published 26 September 2003

Online at [stacks.iop.org/JPhysCM/15/L623](http://stacks.iop.org/JPhysCM/15/L623)

**Abstract**

We are the first group to succeed in measuring the dynamic structure factor  $S(Q, \omega)$  of liquid Si close to melting using high-resolution inelastic x-ray scattering. The spectra clearly demonstrate the existence of propagating short wavelength modes in the melt with a  $Q$ - $\omega$  relation similar to those in other liquid metal systems. A specific variation of the quasi-elastic line shape with increasing  $Q$  is observed close to the structure factor maximum. This observation is related to the onset of atomic correlations on the sub-picosecond timescale in the vicinity of a metal-to-insulator transition. Such observations have been made previously only in computer simulations of metallic systems with increasing covalent character. Our data provide the first experimental evidence for these ultrashort density correlations.

Liquid (l-) Si shows many unusual properties, which in the past have stimulated intensive experimental and theoretical investigations. In the crystalline phase, Si is a typical semiconductor with diamond structure. Upon melting, it undergoes a semiconductor–metal transition [1] where the density increases by about 10% [1]. This transition is accompanied by significant changes in the local structure: e.g. the coordination number increases from 4 in the solid to about 6.5 in the liquid [2, 3]. Despite the metallic nature, its structural properties are considerably more complicated than in typical simple liquid metals such as the l-alkalis. There, the structure factor  $S(Q)$  can be approximated by simple hard-sphere models, and the coordination number is 10–12. In addition to the low coordination number,  $S(Q)$  of l-Si is characterized by a distinct shoulder on the high- $Q$  side of the first maximum (see figure 3), a feature that cannot be reproduced in a simple hard-sphere approach. Many computer simulation

<sup>4</sup> Author to whom any correspondence should be addressed.

<sup>5</sup> On leave from: Department of Materials Science and Engineering, Graduate School of Engineering, Kyoto University, Kyoto 606-8501, Japan.

studies have been carried out on this system employing empirical potentials with three-body terms [4, 5], pseudopotential theory [6], or more recently *ab initio* techniques [7, 8]. In these studies, many experimental results could nicely be reproduced, and in some cases [5, 7, 8] even dynamical properties as the self-diffusion coefficient or information on the vibrational motion could be obtained. Especially in [7], evolution of electron charges around moving atoms could be visualized, indicating chemical bonds with a very short lifetime ( $<30$  fs), whereas the valence-band electron density of states calculated is remarkably free-electron-like, which is in good agreement with photoemission results [9]. In contrast to the intensive theoretical efforts, experimental investigations on collective microscopic motion have been hindered by the fact that the collective modes in l-Si are out of reach for thermal neutrons due to the fast sound velocity ( $\sim 4000$  m s $^{-1}$  [10]) and the kinematical restrictions of this technique.

We have investigated microscopic particle dynamics in l-Si using high-resolution inelastic x-ray scattering (IXS), and for the first time we have measured the dynamic scattering law  $S(Q, \omega)$  of this liquid system. IXS is a technique that allows the study of the  $Q$  dependence of excitations in the millielectronvolt range, but in contrast to neutron scattering, it has no kinematic restrictions. In the energy range of interest the scattered radiation is entirely coherent; hence, this technique is ideally suited for the investigation of the collective dynamics in liquids and disordered solids.

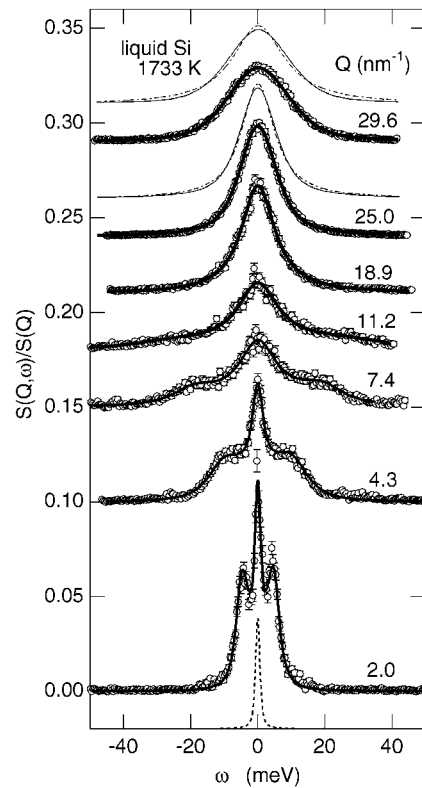
The experiments were carried out at beamline BL-35XU of the SPring-8 using a horizontal IXS spectrometer [11]. A monochromatized beam of  $3 \times 10^9$  photons s $^{-1}$  was obtained from a cryogenically cooled Si(111) double crystal followed by a Si(11 11 11) monochromator operating in backscattering geometry ( $89.975^\circ$ , 21.75 keV). The same backscattering geometry of four two-dimensionally curved Si analysers was used for the energy analysis of the scattered photons. The energy resolution was determined from a Plexiglas sample and values of 1.5–1.9 meV (FWHM) were found for all four detecting systems. The  $Q$  resolution was about  $\pm 0.48$  nm $^{-1}$ . The sample was located in a single-crystal sapphire cell, which was a slight modification of the so-called Tamura-type cell [12]. It was placed in a vessel equipped with continuous Be windows [13] capable of covering scattering angles between  $0^\circ$  and  $25^\circ$ . The high temperature of 1733 K was achieved using a W resistance heater, and monitored with two W–5% Re/W–26% Re thermocouples. The IXS experiments were carried out at 26  $Q$ -values between 2.0 and 29.6 nm $^{-1}$  covering an energy transfer range from  $-50$  to  $+50$  meV. Empty cell measurements were separately performed for background corrections.

Figure 1 shows selected spectra normalized to the integral intensity which is nearly identical to  $S(Q, \omega)/S(Q)$ . Also given is a typical example of the resolution function (dashed curve). The integral intensity of the constant- $Q$  spectra could be normalized using the literature value of  $S(Q)$  [2] measured at the same temperature (see the inset in figure 3). The good agreement demonstrates the high quality of the data.

A resolution correction was accomplished by making use of the fact that the measured intensity is a convolution of  $S(Q, \omega)$  and the experimental resolution function. However, this method requires an appropriate model function for  $S(Q, \omega)$  as an input. We approximated the central line by a Lorentzian at lower  $Q$ -values and as a pseudo-Voigt function at higher  $Q$ -values (see below). The inelastic contribution was approximated by a damped harmonic oscillator (DHO) [14]

$$\left[ \frac{1}{1 - e^{-\hbar\omega/k_B T}} \right] \frac{A_Q}{\pi} \frac{4\omega\Omega_Q\Gamma_Q}{(\omega^2 - \omega_Q^2)^2 + 4\Gamma_Q^2\omega^2}, \quad (1)$$

with  $\Omega_Q = \sqrt{\omega_Q^2 - \Gamma_Q^2}$ .  $A_Q$  and  $\omega_Q$  are the magnitude and energy of the inelastic excitations, and  $\Gamma_Q$  is the width close to HWHM. The solid curves in figure 1 are best fits of the convolution integral to the data.



**Figure 1.** Selected  $S(Q, \omega)$  spectra normalized to  $S(Q)$ . The circles are experimental data and the thick solid curves are fits of the DHO model convoluted with the resolution function (dashed curve). The dotted-dashed curves show fits using a Lorentzian for the quasi-elastic line. They are compared with the results from employing quasi-Voigt functions (thin solid curves, shifted from the data for comparison). See the text for details.

At low  $Q$ , distinct inelastic peaks are visible, which are superimposed by a sharp quasi-elastic line. With increasing  $Q$ , the energy of the excitations rises, indicating that the particle dynamics in l-Si is dominated by propagating modes, as in l-alkali metals [15–19], l-Ge [20, 21], and l-Hg [22].

From the DHO fits, the longitudinal current correlation spectra  $J_1(Q, \omega) = (\omega^2/Q^2)S(Q, \omega)$  were calculated, and the dispersion relation of the collective modes was determined from the maxima  $\omega_1$  of these functions. The result is shown in figure 2, together with the  $Q$ -dependent width of the excitations  $\Gamma_Q$  obtained from the DHO fits. The dashed curve represents the dispersion of hydrodynamic sound. Its slope is given by the bulk adiabatic sound velocity  $c_s = 3952 \text{ m s}^{-1}$  at 1733 K [10]. The frequencies of the collective excitations  $\omega_1$  increase noticeably faster with  $Q$  than predicted by classical hydrodynamics. This is the so-called *positive* dispersion which has already been found in l-alkali metals [15–19], in l-Hg [22] and also in some other l-metals. It can be understood within the framework of extended hydrodynamics [23] and is related to the onset of shear viscosity on microscopic scales at high frequencies [16, 18, 24].

Usually, if the DHO model is employed to match  $S(Q, \omega)$  the quasi-elastic line is approximated by a Lorentzian. However, this choice is not suitable for l-Si beyond  $Q = 20 \text{ nm}^{-1}$ . The tails of the central line decrease much faster than predicted by a Lorentzian.

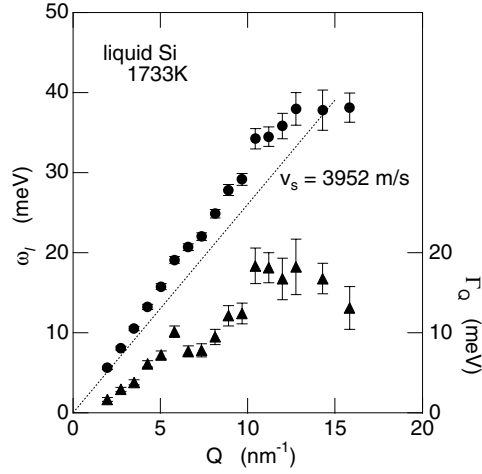


**Figure 2.** Dispersion relation (circles) and line width (triangles) of the collective modes in l-Si. The dashed line gives the dispersion of hydrodynamic sound [10].

Instead, we used a pseudo-Voigt function, which is a weighted combination of a Lorentzian and a Gaussian:

$$\frac{1-c}{\pi} \frac{\Gamma_{0L}}{\Gamma_{0L}^2 + \omega^2} + \frac{c}{\Gamma_{0G}} \sqrt{\frac{\ln 2}{\pi}} \exp\left[-\ln 2 \left(\frac{\omega}{\Gamma_{0G}}\right)^2\right]. \quad (2)$$

Here,  $\Gamma_{0L}$  and  $\Gamma_{0G}$  are HWHM of the Lorentzian and Gaussian, and  $c$  determines the Gaussian fraction. Dotted-dashed curves in figure 1 show the convoluted fits using a Lorentzian in comparison to those using the pseudo-Voigt function (thin solid curves, which are identical to the thicker curves). The pseudo-Voigt function leads to considerably better results than using a pure Lorentzian. The circles and triangles in figure 3 represent  $\Gamma_0$  and  $c$  as a function of  $Q$ . The Gaussian contribution becomes important at around  $20 \text{ nm}^{-1}$  and reaches about 50% at  $Q \sim 30 \text{ nm}^{-1}$ . It is also noteworthy that the so-called de Gennes narrowing of the quasi-elastic line is observed at substantially lower  $Q$  than the position of the maximum in  $S(Q)$ . A similar result was found recently in an *ab initio* MD simulation by Chai *et al* [25].

In order to unravel the physical origin of this unusual line shape behaviour, we have searched for traces of this effect directly in the time domain. Since  $S(Q, \omega)$  is the frequency spectrum of the intermediate scattering function  $F(Q, t)$ , it is possible to obtain the latter from experimental data of sufficient quality. Within the generalized Langevin formalism [26, 27],  $F(Q, t)$  is determined by

$$\ddot{F}(Q, t) + \omega_0^2(Q)F(Q, t) + \int_0^t M(Q, t-t')\dot{F}(Q, t') dt' = 0, \quad (3)$$

where  $\omega_0^2$  is the second normalized frequency moment of  $S(Q, \omega)$  and  $M(Q, t)$  is the memory function of  $F(Q, t)$ . For  $M(Q, t)$ , we used a well-known approximation containing two exponential decay channels for viscous relaxation and one exponential for thermal relaxation. This approach has proven to be useful in describing results of computer simulation studies on simple liquids [28], and also more recently of experimental IXS data on l-alkali metals [19]. For each  $Q$ -value, the real part of the Laplace-Fourier transform of (3) convoluted with the experimental resolution was fitted to our  $S(Q, \omega)$ . It is important to note that the results of this fitting procedure are nearly indistinguishable from the outcome of those fits where Lorentzian

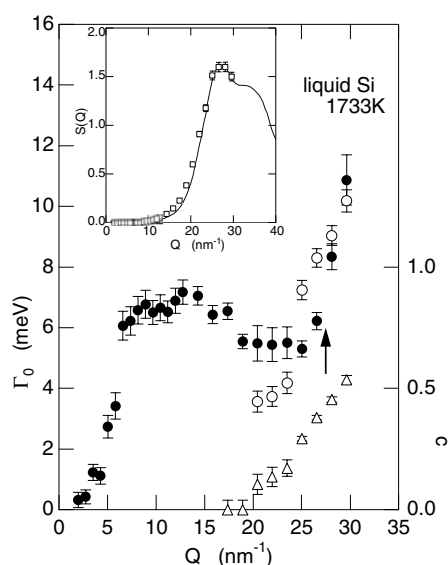


**Figure 3.**  $Q$ -dependence of the quasi-elastic line width  $\Gamma_0$  (circles). With increasing  $Q$ , a Gaussian component ( $\circ$ ) is needed in addition to a Lorentzian ( $\bullet$ ). The triangles indicate the Gaussian fraction,  $c$ . See the text for details. The arrow marks the  $Q$  position of the first maximum in  $S(Q)$ . Inset:  $S(Q)$  determined from the zero-frequency moment of the spectra (squares) together with the result from  $S(Q)$ -measurements [2] (solid curve).

and pseudo-Voigt functions were employed to model the quasi-elastic contribution (solid curves in figure 1). Figure 4 shows selected  $F(Q, t)$  spectra obtained by Fourier transforming the resulting  $S(Q, \omega)$ . They are normalized to their initial values  $F(Q, 0) = S(Q)$ . At low  $Q$  the spectra exhibit oscillatory behaviour, which is the time-domain analogue of the inelastic excitations in  $S(Q, \omega)$ . At  $18.9 \text{ nm}^{-1}$ , the decay of  $F(Q, t)$  is nearly exponential, which reflects the Lorentzian shape of the quasi-elastic line in  $S(Q, \omega)$  in this  $Q$ -range. Close to the  $S(Q)$  maximum, however, it is evident that the decay is no longer exponential. Below  $t = 0.1 \text{ ps}$ ,  $F(Q, t)$  is rather Gaussian, which is in accord with the observation that a Gaussian contribution is needed to model the quasi-elastic line. We interpret the associated slower initial decay of  $F(Q, t)$  as an indication for an additional enhancement of the correlation time between neighbouring particles on the sub-picosecond level. We can also estimate the timescale of the corresponding correlation from  $\Gamma_{0G} \sim 8.5 \text{ meV}$  at the  $S(Q)$  maximum to be  $1/\Gamma_{0G} \sim 0.08 \text{ ps}$ .

It should be noted that this contribution sets in at  $Q$ -values in the vicinity of the  $S(Q)$  maximum where structural correlations to next neighbouring particles dominate. Such short time correlations between neighbours have already been observed in *ab initio* MD simulations [7] on l-Si under similar conditions and interpreted as *striking evidence for the persistence of covalent bonds in the liquid*. In this MD work it was found that on a timescale of some ten femtoseconds a substantial amount of charge piles up between atoms approaching closer than a critical distance  $r_c$ . Interestingly, it was furthermore shown that the bond angle distribution function of these short-lived species peaked at an angle close to tetrahedral, similar to amorphous Si, although there the bond angle distribution is considerably narrower. In a later study, the MD findings were confirmed [8], and it could be shown that localising spins play an important role in the attractive interactions between the Si atoms. These results are in accord with the line shape variation found in our experiment close to the  $S(Q)$  maximum. Also, the estimated correlation period lies in the same range as the timescale observed in the

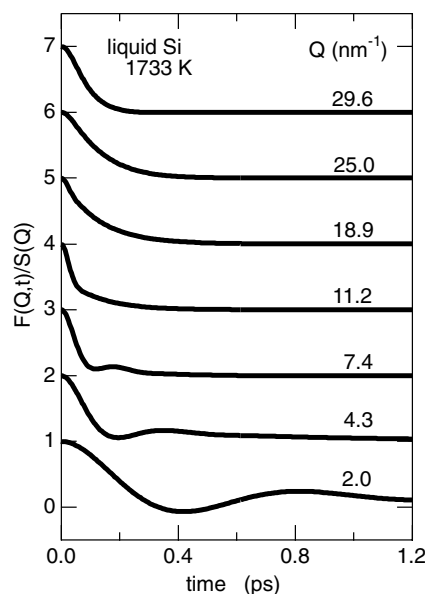


**Figure 4.** The intermediate scattering function,  $F(Q, t)$ , normalized to the initial value  $S(Q)$  at selected  $Q$ -values.

MD simulations. Our observation is therefore the first direct experimental evidence for these sub-picosecond fluctuations.

It is furthermore tempting to speculate that these short time fluctuations of forming and breaking bonds may be interpreted as a precursor of the electron localisation that takes place either on freezing but more likely during the bond formation process when the undercooled metallic Si-melt transforms into a semiconducting amorphous fourfold coordinated state at lower temperature.

The authors acknowledge Professor K Tamura for leaving us his heating equipment during the experiment. This work was performed at the SPring-8 with the approval of the Japan Synchrotron Radiation Research Institute (JASRI) (Proposal No 2002A0182-ND3-np), and supported by the Fonds der Chemischen Industrie.

## References

- [1] Glazov V M *et al* 1969 *Liquid Semiconductors* (New York: Plenum) chapter 3
- [2] Waseda Y and Suzuki K 1975 *Z. Phys. B* **20** 339
- [3] Gabathuler J P and Steeb S 1979 *Z. Naturf. a* **34** 1314
- [4] Stillinger F H and Weber T A 1985 *Phys. Rev. B* **31** 5262
- [5] Broughton J Q and Li X P 1987 *Phys. Rev. B* **35** 9120
- [6] Jank W and Hafner J 1990 *Phys. Rev. B* **41** 1497
- [7] Štich I *et al* 1991 *Phys. Rev. B* **44** 4262
- [8] Štich I *et al* 1996 *Phys. Rev. Lett.* **76** 2077
- [9] Gantner G *et al* 1995 *Europhys. Lett.* **31** 163
- [10] Yoshimoto N *et al* 1996 *Physica B* **219/220** 623
- [11] Baron A Q R *et al* 2000 *J. Phys. Chem. Solids* **61** 461
- [12] Tamura K *et al* 1999 *Rev. Sci. Instrum.* **70** 144
- [13] Hosokawa S and Pilgrim W-C 2001 *Rev. Sci. Instrum.* **72** 1721
- [14] Fåk B and Dorner B 1992 *Institut Laue-Langevin Report* 92FA008S

- 
- [15] Copley J R D and Rowe J M 1973 *Phys. Rev. A* **9** 1656
  - [16] Bodensteiner T *et al* 1992 *Phys. Rev. A* **45** 5709
  - [17] Sinn H *et al* 1997 *Phys. Rev. Lett.* **78** 1715
  - [18] Pilgrim W-C *et al* 1999 *J. Non-Cryst. Solids* **250–252** 96
  - [19] Scopigno T *et al* 2000 *J. Phys.: Condens. Matter* **12** 8009  
Scopigno T *et al* 2002 *Phys. Rev. E* **65** 031205
  - [20] Hosokawa S *et al* 2001 *Phys. Rev. B* **63** 134205
  - [21] Hosokawa S *et al* 2002 *Physica B* **316/317** 610
  - [22] Hosokawa S *et al* 2002 *J. Non-Cryst. Solids* **312–314** 163
  - [23] Boon J P and Yip S 1980 *Molecular Hydrodynamics* (New York: McGraw-Hill)
  - [24] Morkel Chr *et al* 1992 *Phys. Rev. E* **47** 2575
  - [25] Chai J-D *et al* 2003 *Phys. Rev. B* **67** 104205
  - [26] Mori H 1965 *Prog. Theor. Phys.* **33** 423
  - [27] Zwanzig R 1963 *J. Chem. Phys.* **39** 1714
  - [28] Levesque D *et al* 1973 *Phys. Rev. A* **7** 1690